ÉCOLE
POLYTECHNIQUE
DE LOUVAIN

LELEC2710 : Project report

Magnetoconductance oscillations in graphene antidot arrays

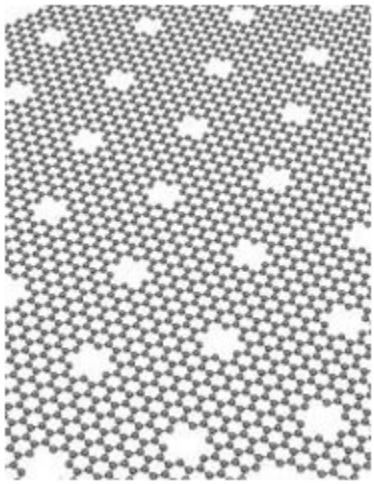

Academic Year 2018-2019
Nanoelectronics

Fievez Thibault - 2545-1500
Santacatterina Simon - 2156-1500

Contents

1 Introduction and goals

Graphene has been the target of numerous researches for that past decade due to its very promising electrical caracteristics. Graphite is simply a monolayer of graphene, which is what pencils are made of, so in other words it is a simple layer of carbon arranged in a hexagonal lattice also called honeycomb lattice. One of the most important caracteristic of graphene is that its conduction band and valence band meet at the dirac points, it therefore means it does not have any band gap. Graphene is also a semimetal because it has a very small overlap between the bottom of the conduction band and the top of the valence band.

Due to its incredible electrical properties, such as displaying a remarkable electron mobility at room temperature [1], an electron and hole mobility expected to be nearly identical and independant of the temperature or its very good thermal conductivity, the interest of using graphene in electrical application become substantial. However, as a semimetal, graphene is not suitable for that. Along with this, the possibility to create a finite, artificial bandgap would be crucial. This could be done using antidot arrays which impose a lateral potential barriers.

The subject of this paper, which is the study of magnetoconductance oscillation in graphene antidot arrays[2], can be considered as a brick in a wall with respect to the end goal, a necessary step to further understand the properties and behaviour of tuned graphene in order to reach particular specification. To help modelizing the effect of the different parameters or geometrical shapes of the lattice on our magnetoconductance KWANT, a quantum effect simulator, will be used.

To be able to fully get a grasp of the whole subjet, the first part of the report will quickly review the most important features and properties of graphene. The different features of the magnetoconductance will then be pointed out and analysed through their effect and causes. And finally, the simulation will be presented.

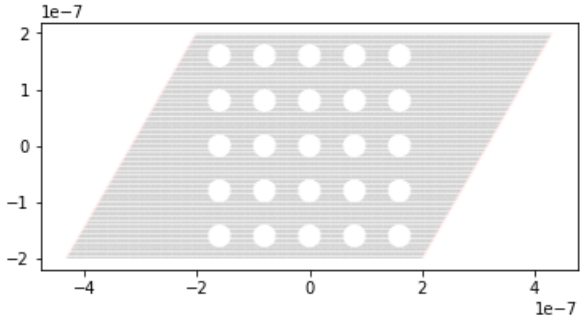

Figure 1: Kwant simulation of an antidot array.

2 The graphene

Graphene is a "crystalline allotrope" [3] of carbon with 2-dimentional properties, it is a 2-D planar layer of honeycomb lattices in which each atom has 4 bonds (3 σ-bond with its neighbours, and one π-bond sticking out of the plane) with inter atom distance of about 1.42 Å.

As stated in the introduction, graphene displays the very unique properties such as being a zero-gap semiconductor, but only when the structure of the nanoribbon is "zig-zag", this does not apply for armchair electronic structures. Indeed it's conduction and valence band meet on the edge of the Brillouin zone, at two specific sets of

[1] With reported values in excess of 15000 $cm^2V^{-1}s^{-1}$ while only 450 $cm^2V^{-1}s^{-1}$ for silicon

[2] An antidot array is simply a sheet of material periodically perforated as shwon on figure 1

[3] An allotrope is the property of certain chemical compounds to exist in various forms. Here are some examples provided by wipikedia: [1] The allotropes of carbon include diamond (the carbon atoms are bonded together in a tetrahedral lattice arrangement), graphite (the carbon atoms are bonded together in sheets of a hexagonal lattice), graphene (single sheets of graphite), and fullerenes (the carbon atoms are bonded together in spherical, tubular, or ellipsoidal formations).

points called K and $K^{'}$. The Brillouin zone is a specific way to divide a reciprocal lattice, the reciprocal lattice represents the Fourier transform of the the real "physical" lattice existing in the "physical" position space. Therefore the reciprocal lattice and Brillouin zone exist in the "reciprocal space" (also called as momentum space). The Brillouin zone is divided in critical point of interest, with a full table available on figure 2.

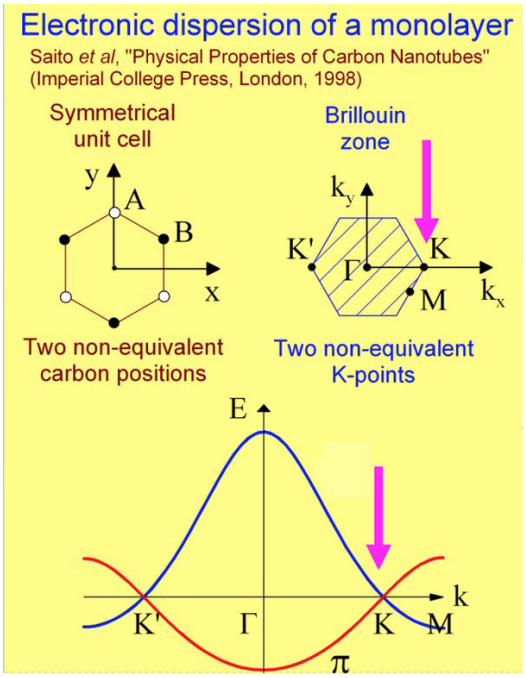

Symbol	Description
Γ	Center of the Brillouin zone
Simple cube	
M	Center of an edge
R	Corner point
X	Center of a face
Face-centered cubic	
K	Middle of an edge joining two hexagonal faces
L	Center of a hexagonal face
U	Middle of an edge joining a hexagonal and a square face
W	Corner point
X	Center of a square face
Body-centered cubic	
H	Corner point joining four edges
N	Center of a face
P	Corner point joining three edges
Hexagonal	
A	Center of a hexagonal face
H	Corner point
K	Middle of an edge joining two rectangular faces
L	Middle of an edge joining a hexagonal and a rectangular face
M	Center of a rectangular face

Figure 2: Visualisation of the Brillouin zone of Graphene and its 2 dirac point where the conduction and valence band meet. [2] [3]

Having two valleys, means that there is 2 contributions to the transmittance as well as no bandgap for both K and $K^{'}$ wave vectors, this step of 2 in transmittance unit can also be visualised on the simulation carried out with Kwant on figure 3 .

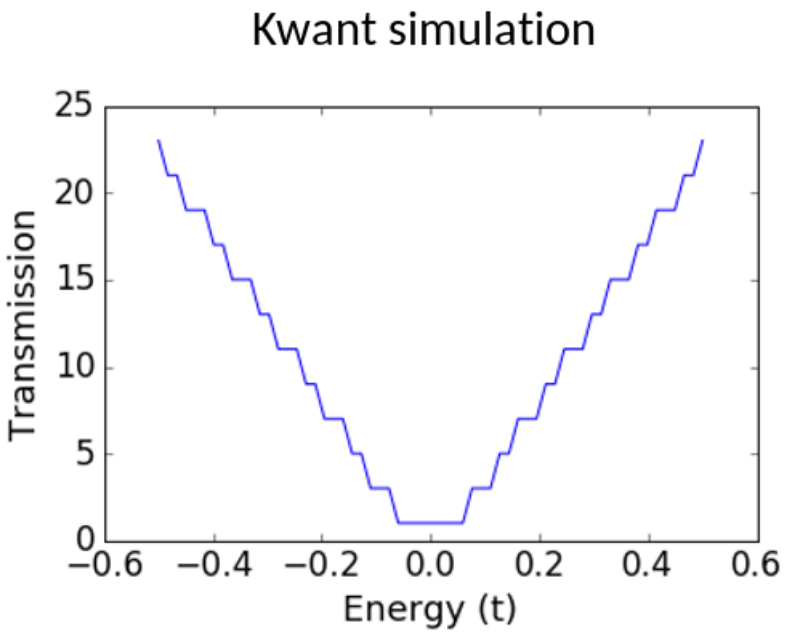

Figure 3: Transmission Simulation with Kwant, clearly, a jump of 2 transmission unit can be noticed in each step, this simulation differ from the others (figure 5) simply by the scaling.

By zooming closer to the meeting point of the conduction and valence bands, so around the pink arrow on figure 2, a specific shape called the Dirac Cone appears as shown on figure 4 .

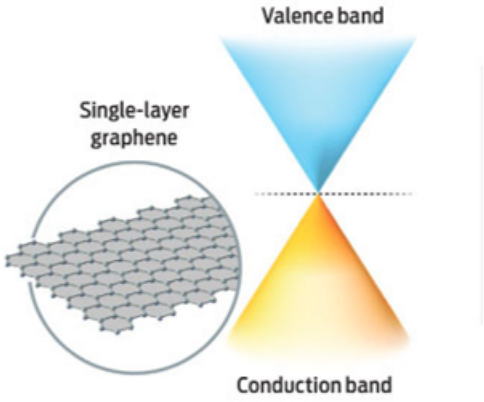

Figure 4: Dirac Cone representation [4]

In practice, the shape may look closer to something like what is displayed on figure 5 .

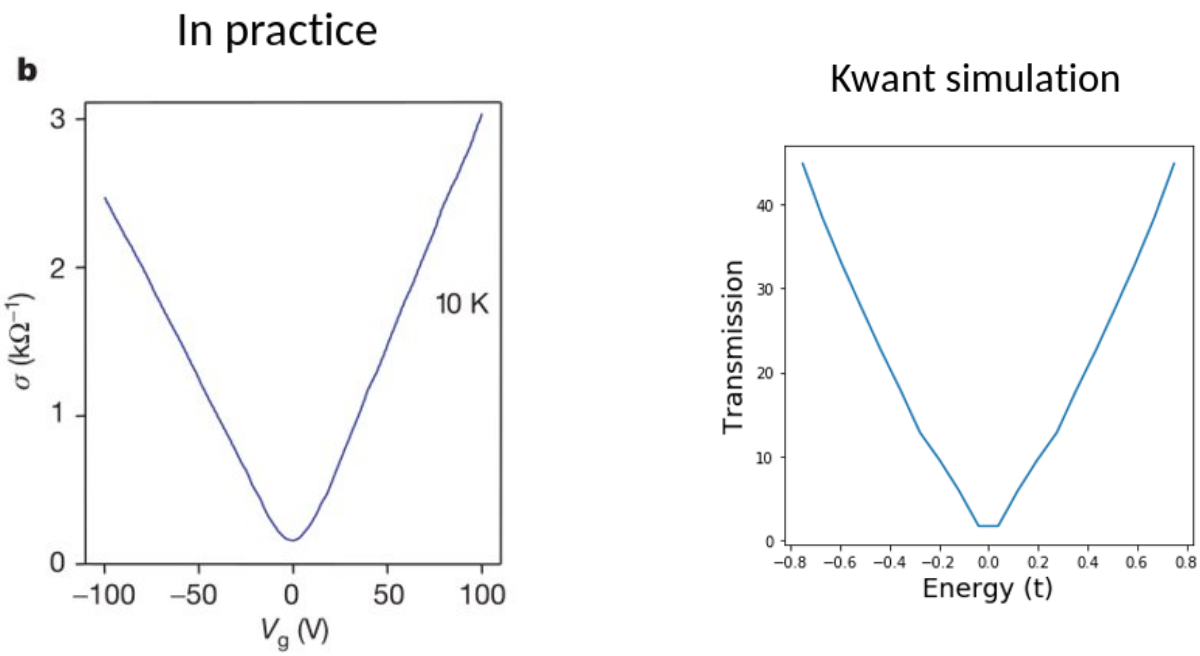

Figure 5: Dirac cone visualization , in practice (from the 2005 paper [5]) and through Kwant simulations

Those Dirac cones are direclty linked to one amazing property of Graphene, which is that it has electrons on the fermi level with a null apparent mass. Indeed , knowing that $E = \hbar k v$ and $m^* = (\frac{\delta^2 E}{\delta^2 k})^{-1}$, and by the fact that the dirac cones have linear slopes, the second derivative of E by respect to k is equal to 0[4]. Those electron that are "losing their mass" are called massless dirac fermions. [5] This means that those electrons do not have inertia and behave like particles that would be traveling at the speed of light according to the theory of relativity. Finally, Graphene has the particularity to have a quantum hall effect can be measured at room temperature and obviously under a magnetic field.

To begin with, some simulations were carried out on a monolayer of graphene with a hole punched in it, this was simply a first step to compare if any of the previous results would change, if that were the case that would mean we would have committed a mistake in our simulations. As expected the same properties of graphene were observed, there was simply a greater resistivity in the sheet with a hole. The results of those simulation can be found on figure 6.

[4]In other materials, comparing the energy E of the electron with respect to the impulsion k, the curve obtained give some sort of parabola, with a curve specific to the material, the second derivative is therefore not null.

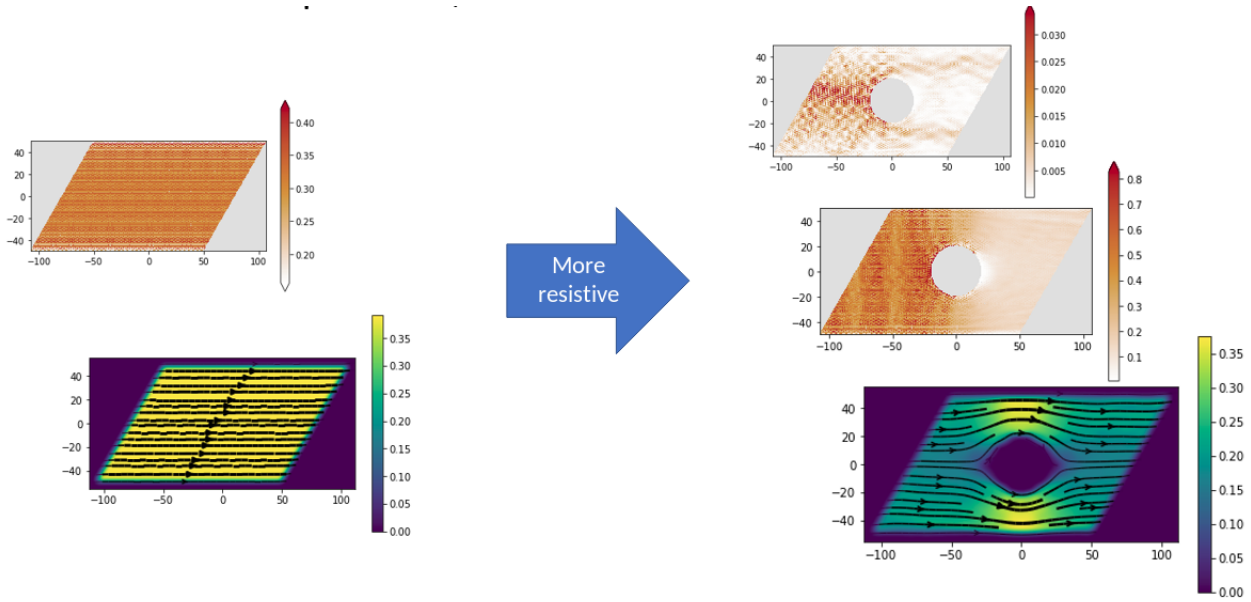

Figure 6: Simulation of a graphene monolayer , the top ones being the density of states (in the very right corner the density of state for the first mode), and the bottom one the current density

3 Magnetoconductance oscillation in graphene antidot arrays

This section will be dedicated to analyze the main subject of the paper which is the quantum hall effect (QHE), or more precisely the magnetoconductance, on a antidot array punched through a monolayer of graphene. The result of the experimentation carried out by the authors of the studied article give the following curve (figure 7). Three main particularities can be observed: weak localization, carriers effect (at 1 and 4) and the Aharonov-Bohm effect. The general shape is coherent with a normal quantum hall effect experimentation for graphene.

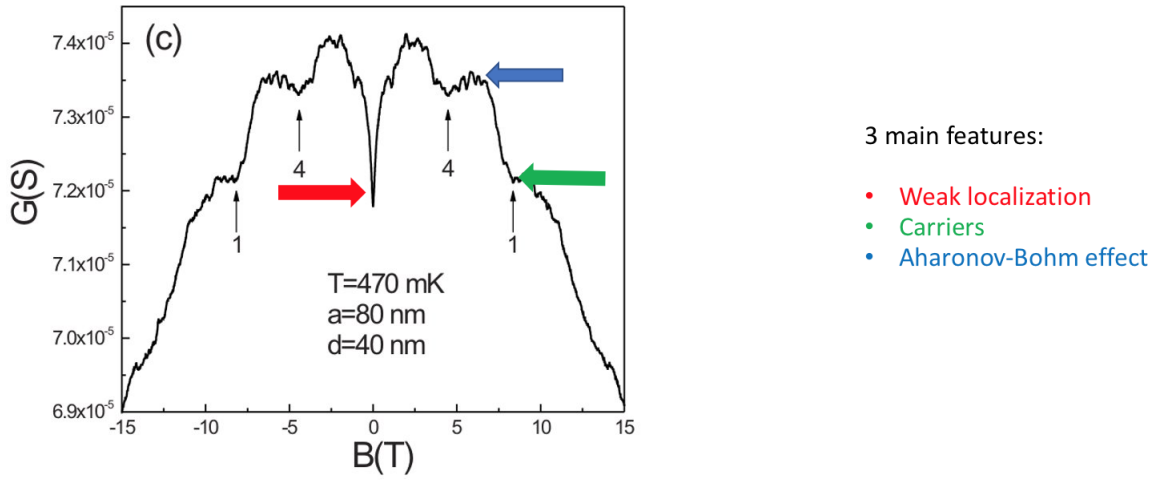

Figure 7: Magnetoconductance of an antidot array. With the 3 main effects highlighted. Graph from the paper of interest [6]

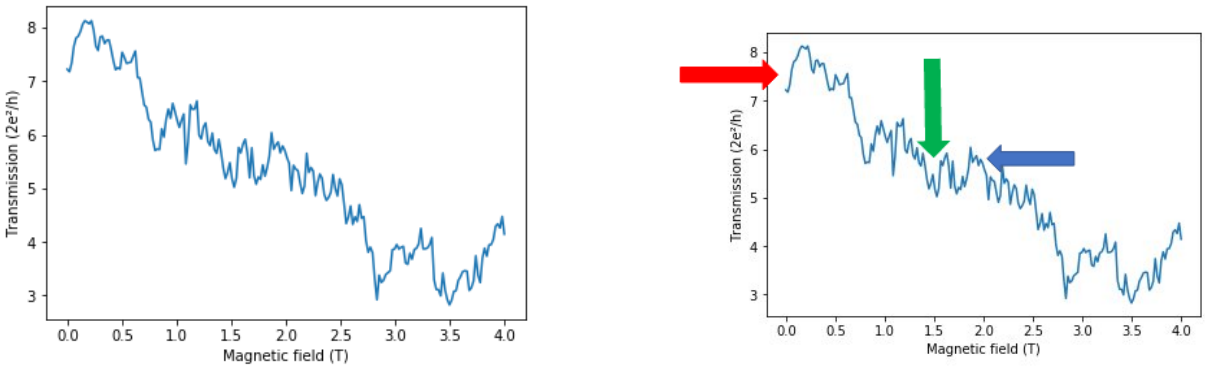

Figure 8: Magnetoconductance of an antidot array through Kwant simulation, only with positive B field. On this graph, weak localzation, 3 distinct levels as well as the carriers effects (around 1.5 and 3.5 T) can be distinguished.

3.1 Weak Localization

3.1.1 Weak antilocalization

While figure 7 clearly exhibits weak localization because of the antidot geometry, natural graphene (loosely coupled to the substrate) behave in the opposite way and exhibits weak antilocalization. While moving in the clockwise path, the pseudospin of the electrons acquires a shift of $-\pi$ whereas in the counterclockwise path the phase shift is π. Then the total shift between the path is 2π, a value for which electron's wave function doesn't returns to its original state. Because of destructive interference, backscattering are suppressed and we have a net increase in conductance. [7]

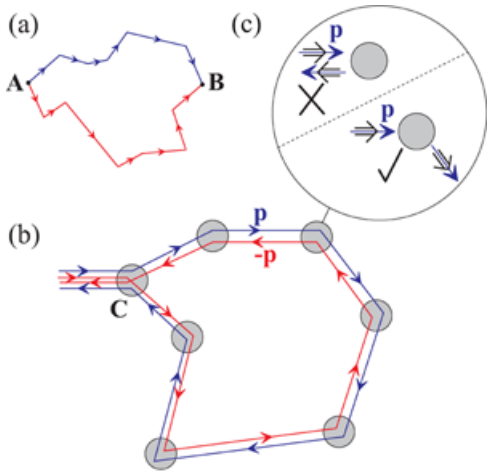

Figure 9: a) Two classical path. b) Electrons moving clockwise and counterclockwise. c) Suppression of back scattering associated with weak antilocalization [7]

3.1.2 Weak localization

The nature of weak localization comes from the disorder of a system, in which the electron has a motion that is closer to diffusion rather than ballistic. [8] In other words, the electron is more likely going to scatter around impurities instead of propagating in a straight line.

The resistivity [5] of a system is related to the probability of an electron to travel from a point A to a point B. In classical physics, that probability is simply the sum of each path's probability that are connecting the two points. However, quantum mechanics tells us that there is another term to add to the equation, which represents the interference between the possible paths. It is those terms that actually make it more likely that a electron will effectively be more likely to wander around some impurities and thus appear to be more localized. This is consistent with the fact that there is a dip in the conductance around 0 tesla as those "trapped" electrons do not contribute to the transmission. This effect quickly disappears as B slightly increases simply because the interference between a clockwise and anti clockwise path is no longer constructive due to the different phase shift induced by the magnetic field.

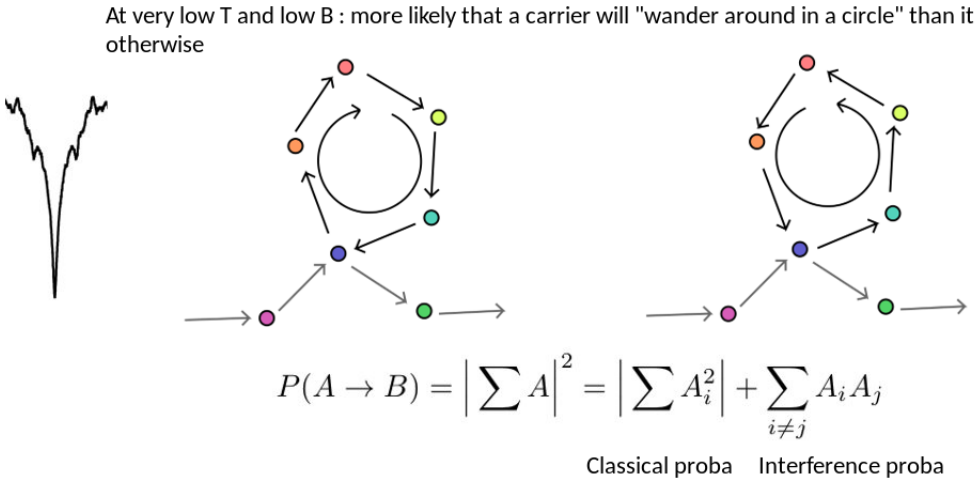

Figure 10: Weak Localization , quickly dissapears as the magnetic filed increases. Source [8]

3.1.3 Weak localization in graphene antidot arrays

Because of the way our antidot is built the weak localization is restored. This is due to three features: short range scattering in epitaxial graphene due to tight binding to the substrate, short range scattering on the edge of the structure and intervalley scattering because of warpping of the Fermy surface at high density. It then creates a peak of magnetoresistance shown on figure 11.

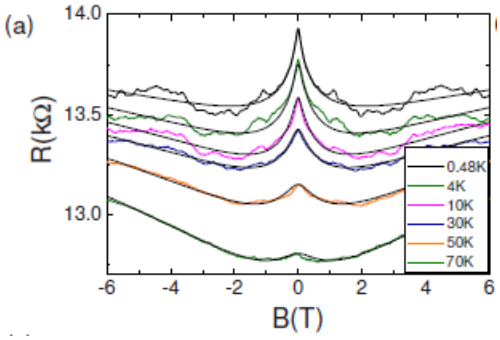

Figure 11: The black curve fot T = 0.48K is consistent with figure 7 and those curves display magnetoresistance for several temperatures

[5] Which is inversely proportional to the conductance

3.2 Carriers

According to the paper of interest, the smaller dips highlighted on figure 7 at 4 and 8 teslas are caused by the three different types of carriers involved: the pinned, scattered and drifting carriers. As one can expect, the pinned carriers do not contribute in anyway to the transmission and those are the main cause of the dip in conductance. This effect is purely geometric and related to the periodicity of the pattern, the hole's radius, and the magnetic field applied.

As shown on figure 12, an electron under a magnetic field feels a force given by $F = ev \times B$, and as such it has a cyclotron frequency given by $\omega_c = |\frac{eB}{m}|$, from that, it's cyclotron radius can be found such that $R_c = \frac{v}{\omega_c} = \frac{\sqrt{2mE}}{|eB|}$ with v the linear speed of the electron.In the studied paper, [6]this formula can be expressed as $R_c = \sqrt{\pi N_s}(\frac{\hbar}{eB})$ when the cyclotron radius is equal to half of the period of the antidot array. Which means an electron would start spinning in a circle of radius R_c if it didn't encounter any obstacles. A electron becomes pinned when it's cyclotron radius matches one or many holes (n^2 where n = 1,2,3, ...) from the antidot array, it is "trapped" and start circling around this/those dot(s). The reason why this effect appears periodically as B changes can be understood quite simply by an example: let's imagine an electron that would originaly be spinning around 9 holes (for a certain B), when B will increase there will be a point when the electron would have a cyclotron radius that would enable him to rotate around 4 dots, it will therefore be pinned once again.

The others kind of carriers have a lesser visible impact on the graph of the magnetoconductance even if it important to realize that those are actually the ones that contributes to the conductance. These two categories are the s (or scattering carriers) travelling as a ballistic transport between collisions with a big cyclotron radius and the d (or drifting carriers) travelling in circle without being trapped around any holes characterized by a small cyclotron radius. A variation in B simply causes a variation in the proportion between the different types of carrier. These facts are displayed on figure 12.

The effect of pinned carriers has been observed for the simulation conducted with Kwant, its visualisation is avalaible on figure 13 .

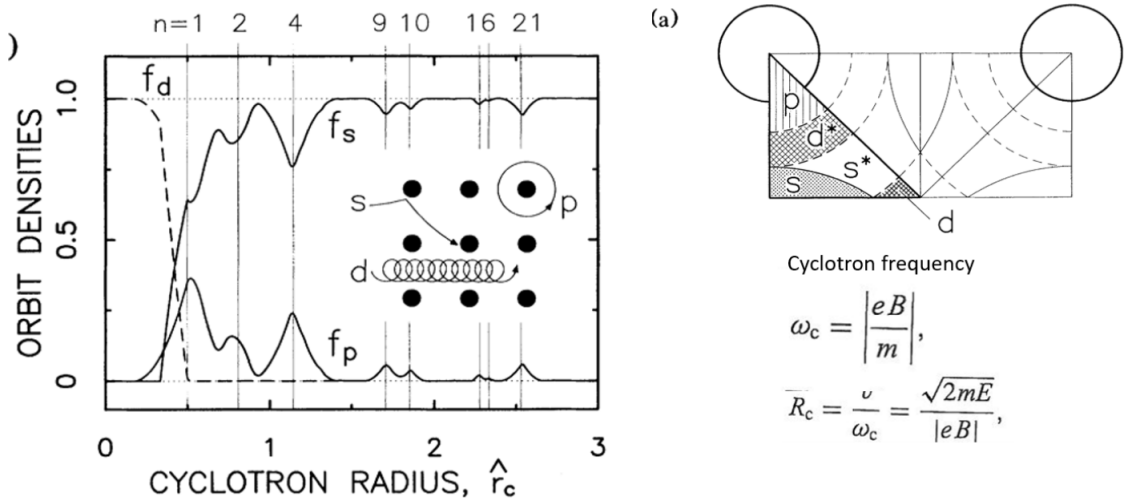

Figure 12: The different types of carriers, with their cyclotron radius distributions on the left. And their region of travelling on the right [9]

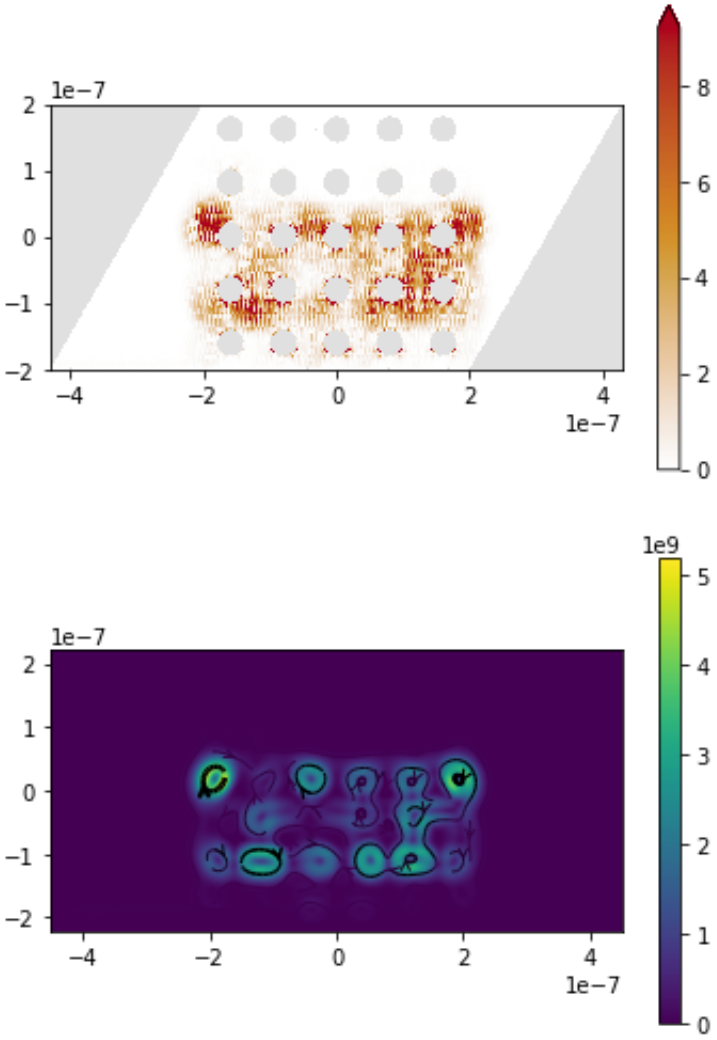

Figure 13: Visualization of the Pinned orbits through simulations, the top pictures being the total density of state and the bottom on the current density.

3.3 Aharonov-Bohm

3.3.1 General explanation and implications

Aharonov-Bohm oscillations in conductance are seen in blue on figure 7. Those oscillation can be associated with the Aharonov-Bohm effect, as stated in the paper of interest. [6] The universal conductance fluctuations are suppressed since the sample size is much larger than the phase coherence length. Indeed, for each holes of our array, a magnetic flux is created by the crossing of the field through the holes surfaces. While electrons are travelling around these holes they are then subject to the a similar effect as if they were travelling through an Aharonov-Bohm ring as shown on the left of figure 14.

Even if outside the holes the magnetic field is zero the vector potential $\mathbf{A}$ is present and will affect the electron's phase near the hole. Actually, electrons enter in the loop around holes, divide in two path, undergo different phase shift and recombine while exiting the ring. The momentum $\hbar\mathbf{k} = \mathbf{p} + e\mathbf{A}$ stays constant but $\mathbf{p}$, acting directly on the phase, changes because of the value of $\mathbf{A}$. We have $\hbar\mathbf{k}$ - $e\mathbf{A} = \mathbf{p}$. Then for the crossing through the top branch, because $\mathbf{A}$ and $\mathbf{k}$ are opposite $\mathbf{p}$ increases while the opposite happens on the bottom. [10] The difference in phase

between the two path is given by:

$$\Delta\phi = (e/\hbar)\Phi = 2\pi(\Phi/\Phi_0)$$

Where $\Phi_0 = h/e$ is the quantum of flux, which quantifies the flux. And because $G \propto \cos^2(\pi\Phi/\Phi_0)$ We have periodic conductance oscillations as displayed on the right on figure 14.

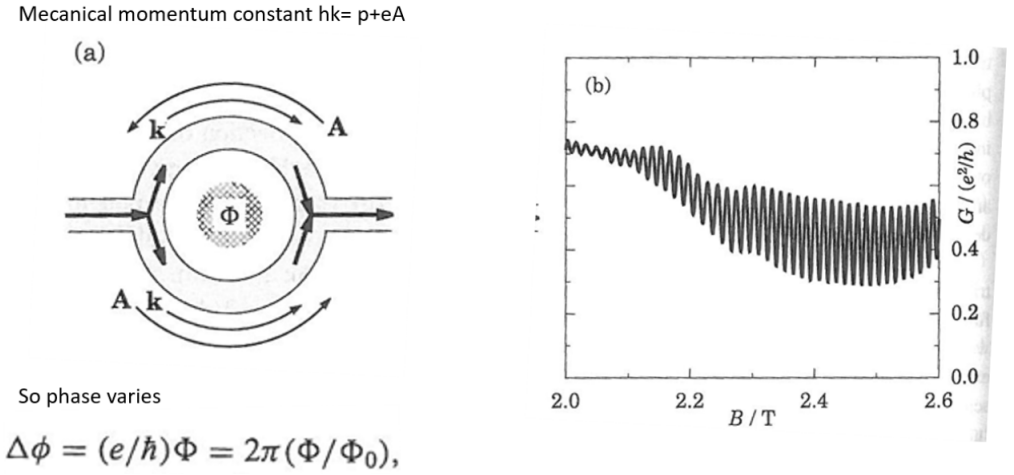

Figure 14: AB effect [10]

3.3.2 Experimental results from the paper

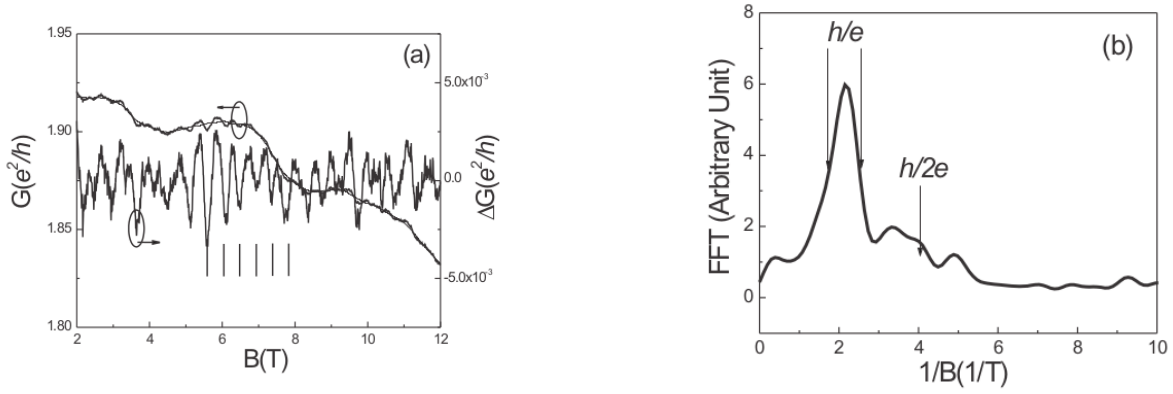

Figure 15: AB oscillations for the antidot from the paper on the left and its associated power spectrum on the right

The periodicity of the oscillation can then be explained using the theory above. Because the ΔB is small (around 0.5T) it can be assume that for a unit cell the magnetic flux increases by a single quantum flux. This means $\Delta B = (h/e)/a^2 \approx 0.5T$. This is congruent with the FFT for which we can see that most of the power of these AB oscillation (the highest peak) is located at field 1/B = 2 (1/T) or B = 0.5T.

3.4 Overview of the Quantum Hall Effect

The general shape of the curve of the Magnetoconductance is due to the Quantum Hall effect. A general comparison is available on figure 16

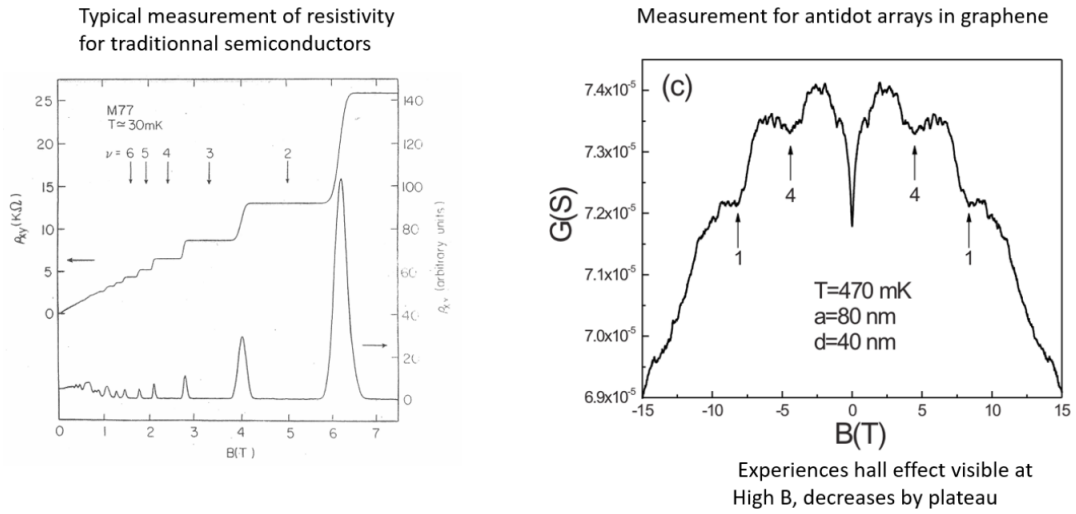

Figure 16: Comparison between a classical graph of QHE [11] and for the antidot array in graphene, [6] it is important to realise that the scale of the left hand side graph is the resistivity whereas the right hand side is the conductance.

The quantum hall effect is due to the crossing of the Fermi energy level with the landau's level. The more landau level the fermi energy "line" (see figure17) crosses, the better the conductance is. As the magnetic field increases the spacing between the landau levels increases whereas the fermi energy remains constant. A bigger spacing between those levels means that the fermi energy line might not cross as many landau levels as with a lower magnetic field and therefore the magnetoconductance decreases. This induce the general shape of the curves in figure 16, the plateau is the "in between" case when the fermi energy is constant and the spacing between the plateau increases and each significant decrease in the curve is due to the fact that the fermi energy level crosses and goes beneath one more landau level. This can also be visualized on the simulation carried out on Kwant on figure 18.

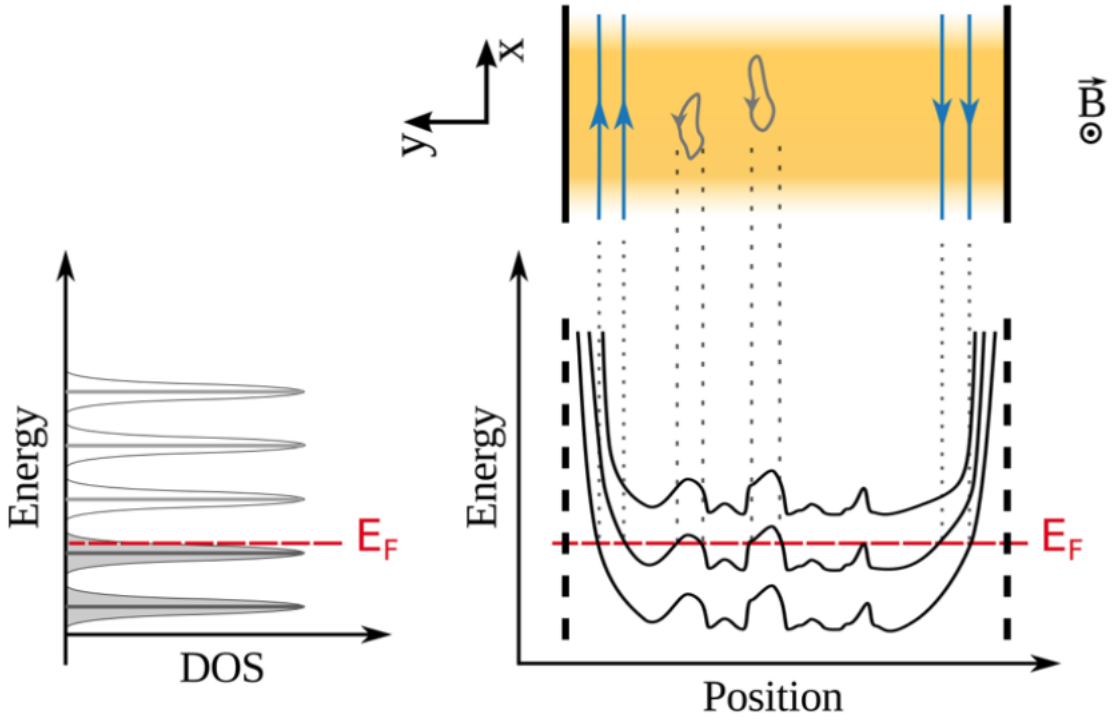

Figure 17: Laudau levels visualization

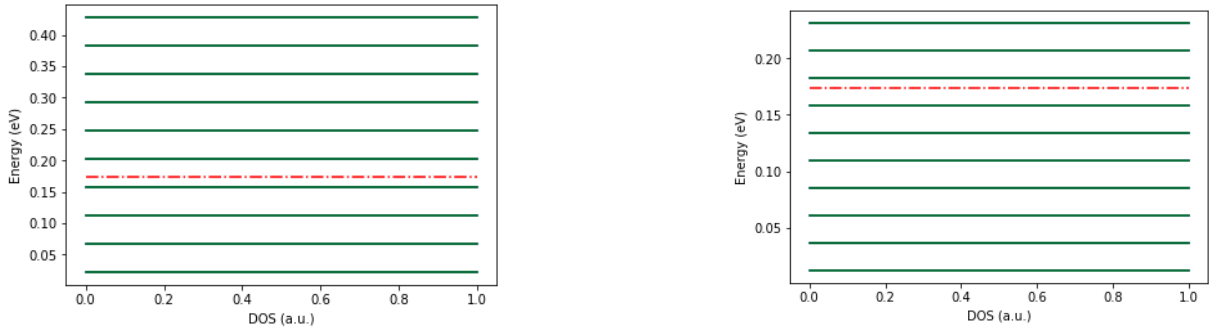

Figure 18: Laudau levels simulation on Kwant with the fermi energy in red, with B=3.7T on the left figure and B=2T for the right figure. As expected the fermi energy doesn't vary but the spacing between the landau level does.

4 Kwant Simulation

This section highlight the most important part of the code, the full code will also be provided with this report. The scaling was adapted to the system studied. [12]

```
a = 2e-9 ; t = 1 # the lattice parameter and the hopping energy # graphene a= 1.42 e-10
W = 400e-9 ; L = 400e-9 # width and length of the electronic system

#### if you need a proper scaling to find the Fermi energy (a should be the real value) in AlGaAs/GaAs systems ####
n2D = 2.4e15 # electronic density of the 2 dimensional electron gas in Graphene
vf=10**6 # =10**6 by wallace or 3*t*a / 2
#https://www.google.com/url?sa=t&rct=j&q=&esrc=s&source=web&cd=2&ved=2ahUKEwj9lLbpq6nfAhUDjqQKHby8CigQFjABegQICBAC&url=htt

Ef = a*(np.pi*n2D)**(1/2) # reference provided paper from shen
#2*np.pi * t * a**2 * n2D # Fermi energy computed from the electronic density
print(Ef)
```

```
#### For a realistic value of phi ####
B = 2 # (Tesla) value of the magnetic field (well, the magnetic flux density for the purists among you)
phi = B/(2*h)*3*e*(3**(1/2))*(a**2)     #B * a**2 # with 'a' being a realistic value (below the nanometer)
print(phi)
```

Figure 19: Sizing and dimensions

- How to draw the shape

```
def geom(pos):
    x, y = pos
    number = 4
    r1 = 20e-9
    if -L/2 < x < L/2 and -W/2 < y < W/2:
        for up in range(-number//2,1+number//2):
            for right in range(-number//2,1+number//2):
                center = ((80e-9*up),(80e-9*right))
                rsq = (x-center[0])** 2 + (y-center[1])** 2
                if r1**2 > rsq:
                    return False
                else:
                    c = True
        return c
```

- How to include the effect of a Magnetic Field (on the phase)

```
def hopping(site_i, site_j, params):
    """
    Definition of the hopping parameter by including the magnetic field (parameter phi)

    """

    xi, yi = site_i.pos
    xj, yj = site_j.pos

    #### For a value of phi adapted to the system - definition adopted in the Kwant documentation
    return -t * exp(-1j * np.pi * phi / (h/e) * (xi - xj) * (yi + yj)/a**2)
```

Figure 20: Drawing of the Shape and adding the magnetic field

Computation of the local electronic density

```
wfs = kwant.wave_function(sys, energy=Ef, args=[params]) # the wave function is obtained by giving the
                                                         # parameters in arguments
scattering_wf = wfs(0)  # all scattering wave functions from lead 0
kwant.plotter.map(sys, np.sum(abs(scattering_wf)**2, axis=0)) # to map the wave function
```

Computation of the local current density

```
J0 = kwant.operator.Current(sys)
wf_left = wfs(0)
current = sum(J0(p, args=[params]) for p in wf_left) # to sum over all the lead's mode

kwant.plotter.current(sys, current, cmap='viridis')
```

Calculation of the transmission across the system as a function of the magnetic field

```
N = 200 # number of magnetic field values
Bmax = 4 # higher magnetic field
Bs = np.linspace(0, Bmax, N) # vector of the magnetic fields

G = np.zeros([N,1])

for i,B in enumerate(Bs):
    phi = B * a**2
    params = SimpleNamespace(phi=phi)
    smatrix = kwant.smatrix(sys, energy =2*Ef, args=[params]) # transmission matrix (here this)
    T = smatrix.transmission(1, 0) # transmission value obtained from the left lead towards the right lead
    G[i] = T
    print(B,T)
plt.plot(Bs,G)

plt.xlabel('Magnetic field (T)')
plt.ylabel('Transmission (2e²/h)')

plt.show()
```

Computation of the local density of state and the corresponding current density for different magnetic field values

```
Bs = np.linspace(0, Bmax, 10)
for B in Bs:
    print('Magnetic field : ', B, ' (T)')
    phi = B * a**2
    params = SimpleNamespace(phi=phi)
    wfs = kwant.wave_function(sys, energy=Ef,args=[params])
    scattering_wf = wfs(0)  # all scattering wave functions from lead 0
    kwant.plotter.map(sys, np.sum(abs(scattering_wf)**2, axis=0));

    wf_left = wfs(0)
    current = sum(J0(p, args=[params]) for p in wf_left) # to sum over all the lead's mode
    kwant.plotter.current(sys, current, cmap='viridis')
```

Figure 21: Calculations

5 Conclusion

As a conclusion, the different features of magnetoconductance in antidot arrays have been reviewed. Those include weak localization, as opposed to traditional anti weak localization in graphene, the effect of carriers and Aharonov-Bohm oscillations. Traditional quantum hall effect was quickly reviewed. Many curves have not been included in this report for consistency's sake, though, if the reader wishes, the code provided along this paper will enable him to study or observe the effects of the different parameters, this code has been extended and adapted from another code [11] to work as intended for graphene with an antidot array. By default, this adapted code will provide the same results are those displayed in this report.

References

[1] A. N. Author. Wikipedia. *https://en.wikipedia.org/wiki/Allotropy*, 2018.

[2] Edward McCann. Weak localisation magnetoresistance in graphene. *https://www.pks.mpg.de/ coqusy06/SLIDES/mccann.pdf*.

[3] A. N. Author. Wikipedia. *https://en.wikipedia.org/wiki/Brillouin$_z$one*, 2018.

[4] A. N. Propiedas y aplicaciones-electricas del grafeno. *http://www.applynano.com/es/propiedades-y-aplicaciones-electricas-del-grafeno/*, 2018.

[5] S. V. Morozov D. Jiang M. I. Katsnelson I. V. Grigorieva S. V. Dubonos A. A. Firsov K. S. Novoselov, A. K. Geim1. Two-dimensional gas of massless dirac fermions in graphene. 2005.

[6] M. A. Capano L. P. Rokhinson L. W. Engel T. Shen, Y. Q. Wu and P. D. Ye. Magnetoconductance oscillations in graphene antidot arrays. *American Institute of Physics*, 2008.

[7] Edward McCann. Viewpoint: Staying or going? chirality decides! *https://physics.aps.org/articles/v2/98*, 2009.

[8] A. N. Author. Wikipedia. *https://en.wikipedia.org/wiki/Weak$_l$ocalization*, 2018.

[9] A. Menschig P. Grambow K. von Klitzing D. Weiss, M. L. Roukes and G. Weimann. Electron pinball and commensurate orbits in a periodic array of scatterers. *American Physical Society*, 1991.

[10] John H. Davies. The physics of low-dimensional semiconductors. *Cambridge University Press*, 1998.

[11] B. Hackens and V. Bayot. Cours lelec2710: Nanoelectronic. 2018.

[12] K. Kazymyrenko and X. Waintal. Knitting algorithm for calculating green functions in quantum systems. *American Physical Society*, 2008.